REMOVAL OF METHYLENE BLUE DYE USING PALM TRUNK BASED ACTIVATED CARBON VIA MICROWAVE IRRADIATED: OPTIMIZATION, ISOTHERM, KINETIC AND THERMODYNAMIC STUDIES

Mohamad Hafiz Baharudin¹, Mohamad Firdaus Mohamad Yusop¹, Muhammad Nasri Nasehir Khan¹, Muhammad Azan Tamar Jaya² and Mohd Azmier Ahmad^{1,*}

¹School of Chemical Engineering, Universiti Sains Malaysia, Penang, Malaysia ²Kolej GENIUS Insan, Universiti Sains Islam Malaysia, Negeri Sembilan, Malaysia

*chazmier@usm.my

Abstract. Polluting the environment with synthetic dyes can adversely affect humans, animals, and plants. This study aimed to produce optimized palm-trunk-based activated carbon (PTAC) using response surface methodology (RSM) to remove methylene blue (MB) dye. The PTAC was prepared by physical activation with microwave radiation and carbon dioxide (CO₂) gasification. The RSM revealed the optimal PTAC preparations with an activation time of 4 minutes and a radiation power of 501 W, respectively. Optimized PTAC removed 91.25 % of the MB dye, and the PTAC yield was 32.37 %. The Brunauer- Emmett-Teller (BET) surface area of this sample is 772.35 m²/g, the pore volume is 0.45 cm³/g, and the fixed carbon content is 74.30 %. The pores created in PTAC is mesopores type of pores, with an average diameter of 3.88 nm. The Freundlich model performed the best on the adsorption isotherm which signified the multilayer coverage of MB occurred on the surface of PTAC. The maximum monolayer adsorption capacity, Q_m computed from Langmuir model was found to be 312.50 mg/g. In terms of kinetic study, the pseudo-second-order (PSO) model performed the best with rate constant, k₂ decreased from 0.087 to 0.016 g/mg.h when MB initial concentration increased from 25 to 300 mg/L. The thermodynamic study revealed that the adsorption of MB onto PTAC was endothermic in nature ($\triangle H^{\circ} = 34.48 \text{ kJ/mol}$), spontaneous ($\triangle G^{\circ} = -5.22$ to -8.99 kJ/mol) and governed by physisorption (E_a = 7.33 kJ/mol). Therefore, PTAC showed excellent application in dyes wastewater treatment systems.

Keywords: Adsorption, activated carbon, methylene blue, response surface methodology, isotherm, kinetic

Article Info

Received 18th January 2023 Accepted 7th April 2023 Published 1st May 2023

Copyright Malaysian Journal of Microscopy (2023). All rights reserved.

ISSN: 1823-7010, eISSN: 2600-7444

Introduction

One of Malaysia's primary industries is the textile and apparel industry, with 1.7 % of Malaysia's exports going to the United States, the United Kingdom, Japan, and Germany. As the population grows, so does the need for bright clothing. It is estimated that more than 10,000 various type of dyes are produced nowadays [1]. Pre-treatment, polymerization, spinning, texturizing, dyeing, printing, and made-up textile goods are all parts of the textile industry. All these activities use water and cause pollution. In the dyeing process, the primary wastewater sources are spent dye baths and wash water. Besides dyes, textile wastewater contains other harmful substances such as solvents, salts, and others. However, this study mainly focuses on dyes because dyes constitute the highest percentage of textile wastewater which is 30% [2].

Moreover, compared to other substances, textile dyes are the most toxic to aquatic organisms, and they can enter the food chain if not adequately treated, contaminating aquatic habitats [3]. Because the textile industry produces a large amount of highly colored wastewater that contains a diverse range of persistent pollutants, dyes that contain wastewater are a significant polluter of the environment and have an impact on human health [4]. Researchers have attempted to create a few techniques for efficiently extracting dyes from industrial wastewater, including adsorption, membrane filtration, ion exchange, electrochemical, photo-oxidation, coagulation-flocculation, and floatation. However, the high cost and production of hazardous materials limit most of these technologies.

Adsorption is the best way to get rid of dyes based on how well it works, how much it costs to run, and how safe the used adsorbents are [5]. Most adsorption happens through physisorption or chemisorption, which involve weak van der Waals forces and covalent or ionic holding. Also, activated alumina, silica gel, graphene, nanomaterials, activated carbon (AC), and zeolites are the adsorbents used most often in adsorption. AC is the best type of adsorbent for removing a wide range of pollutants such as dyes [6-8], toxic gases [9], heavy metals [10-11], and others from wastewater. AC's precursors can be any carbonaceous item, including coconut shells, wood, agricultural waste, nutshells, and other materials containing amorphous carbon. Adsorbent derived from agricultural waste is preferable because of the raw material's availability, affluence, and renewability.

The palm trunk is a significant biomass waste production from palm oil operations that is to be treated at a low cost. Malaysia is one of the major players in the palm oil business, with 5.90 million hectares of oil palm cultivation land in 2021, generating palm oil and palm kernel oil of 19.86 million tonnes and 2.32 million tonnes, respectively [12]. The industry produces numerous waste products: palm trunks, empty fruit bunch, palm fronds, and palm oil mill effluent (POME). The palm trunk was the focus of this study to investigate its potential to produce activated carbon with the help of microwave radiation. Since this carbon is abundant and exclusively found in the field, it might be used to adsorb dyes from wastewater.

Materials and Methods

Materials

Sigma-Aldrich (M) Sdn Bhd supplied the MB dye (Molecular Formula $C_{16}H_{18}CIN_3S$) to be used as the adsorbate. The MB dye is classified as a basic dye. The precursor of palm trunk was collected from a grove of oil palms in Nibong Tebal, Penang.

Synthesis of PTAC

Initially, the palm trunk was air-dried for several days to remove moisture. The palm trunk was then sliced into 5 mm-thick pieces and dried in an oven for two nights to remove excess moisture. The carbonization process then involved placing the dried palm tree in a furnace. This procedure lasted for 10 minutes at 350 °C. Under a CO₂ flow rate, the microwave-assisted activation treatment was carried out in a modified microwave at the specified power and duration.

Optimization of PTAC's Preparation Conditions

The optimization of PTAC's preparation conditions was created by using a program known as Design-Expert software version 8.0.6 (DOE) by studying two variables: radiation power, x_1 (W), and activation time, x_2 (min). The results were MB elimination, y_1 (percent), and PTAC yield, y_2 . A face-centered composite design (FCD), a standard response surface methodology (RSM) design, was used to investigate the two variables. Table 1 depicts the levels and ranges selected for this study. As determined by the experimental design matrix, the ideal value is 501 W of radiation power for four minutes.

Variables (factors) Coded variables level *-* α -1 0 +1 $+\alpha$ Activation power (watt) 191 264 440 616 689 Activation time (min) 3.17 4.00 6.00 8.00 8.83

 Table 1: Independent Variables for FCD

Batch Adsorption Studies

For the PTAC's adsorption testing, six 250 ml Erlenmeyer flasks were employed, each carrying a different MB dye concentration. Six distinct dye concentrations of 25, 50, 100, 200, 250, and 300 mg/L were produced by diluting the dye with deionized water. After sealing, each Erlenmeyer flask was put in an isothermal water bath shaker for 24 hours at 30 °C and 60 rotations per minute. At spectrum of 665 nm, the UV-Visible spectrometer (Agilent Cary 60, USA) was used to detect the absorbance of the MB dye. By measuring the absorbance rate against the established MB dye concentrations, a previously generated calibration curve was utilized to calculate the concentration of the MB dye. The adsorption data were fitted on several models in both isotherm and kinetic studies. The best model that described the adsorption isotherm data and adsorption kinetic data was the one that produced the highest value of correlation coefficient, R². The R² value is a statistical measure representing the strength of the relationship between two variables. A higher R² value indicates a stronger relationship between the variables and a better fit of the regression line to the data.

Characterization Tests

Characterization of samples in terms of surface area, pore volume, and average pore diameter was conducted using a surface area analyzer (Micromeritics, Model ASAP 2020, USA), where the BET equation was applied to determine the value for BET surface area. The SEM images were taken using Scanning Electron Microscopes (SEM) analyzer (Model Quanta 450 FEG, Netherlands). An electron beam is generated and directed onto the sample. The beam is scanned over the surface of the sample, and a detector collects the electrons that are scattered or emitted from the sample. The alignment of the beam and detector are adjusted to optimize the SEM image quality. Proximate analysis to determine the components of fixed carbon, moisture content, volatile matter, and ash was performed using a thermogravimetric analyzer (TGA) (Model Perkin Elmer STA 6000). Elemental analysis was carried out to detect the elemental of C, H, N, and O using an elemental analyzer (Perkin Elmer Series II 2400, USA).

Results and Discussion

Response Surface Methodology (RSM)

(a) Radiation Power and Activation Time

Table 2 shown that the experimentally determined response values and a comprehensive design matrix for creating PTAC. Analysis of experimental data revealed that MB removal varied between 75.49 % and 98.12 %. Equations 1 and 2 demonstrate how the final empirical models expressed the link between variables and response using factor coding. Positive signs synergistically affect each word, but negative signs have an antagonistic effect. Quadratic models were used for MB removal (Y1) and PTAC yield (Y2) because they revealed a link with the results. The models of empirical formulas for the response in terms of code factor are demonstrated by Equations 1 and 2.

$$Y1 = 97.41 + 6.83x_1 + 4.96x_2 - 3.23x_1x_2 - 5.01x_1^2 - 4.22x_2^2$$
(1)

$$Y2=35.78-5.92x_1+0.10x_2+0.08x_1x_2-0.50x_1^2-1.88x_2^2$$
(2)

The quality of the model was evaluated using the coefficient of determination, R². In this research, the PTAC yield and MB removal R² values were 0.9294 and 0.9397, respectively, close to unity. The experimental data accounted for 92.94 % of the variation in MB removal and 93.97 % of the variation in PTAC yield, according to Equations 1 and 2 above. The sufficiency and applicability of the model were proven using analysis of variance (ANOVA). Table 3 illustrates the ANOVA findings for the quadratic models of PTAC yield and MB removal. The quality of the created model was determined by assessing the Model F-value and Prob> F. Since the Prob> F value for both responses of MB removal and PTAC yield was below 0.05, therefore these models were significant.

Table 2: Experimental Design Matrix for preparation of PTAC

Run	Run Level		PTAC prepar	ation variable	MB	PTAC	
			Activation power, x_1 (W)	Activation time, x ₂ (min)	removal, Y_I (%)	yield, <i>Y</i> ₂ (%)	
1	0	0	440	6.00	98.12	40.2	
2	0	-1.414	440	3.17	77.58	29.7	
3	-1	-1	264	4.00	75.49	40.2	
4	0	0	440	6.00	96.02	35.2	
5	0	0	440	6.00	95.56	35.4	
6	1	1	616	8.00	97.66	28.1	
7	1	-1	616	4.00	98.08	30.1	
8	-1.414	0	191	6.00	77.86	43.5	
9	-1	1	264	8.00	87.98	38.5	
10	0	0	440	6.00	97.22	35.7	
11	0	1.414	440	8.83	97.13	32.9	
12	1.414	0	689	6.00	93.68	24.5	
13	0	0	440	6.00	98.11	36.2	

Table 3: ANOVA table for MB removal and PTAC yield

MB Removal					PTAC Yield					
Source	Sum of squares	Degree of freedom (DF)	Mean square	F- Value	Prob.>F	Sum of squares	Degree of freedom	Mean square	F- Value	Prob.>F
Model	876.45	5	175.29	18.44	0.0007	304.83	5	60.97	21.82	0.0004
x_1	373.23	1	373.23	39.26	< 0.0004	280.49	1	280.49	100.40	< 0.0001
x_2	197.19	1	197.19	20.74	0.0026	0.085	1	0.085	0.030	0.8663
x_1x_2	41.67	1	41.67	4.38	0.0746	0.023	1	0.023	0.42	0.9310
x_1^2	174.52	1	174.52	18.36	0.0036	1.73	1	1.73	0.62	0.4575
x_{2}^{2}	123.66	1	123.6	13.01	0.0087	23.76	1	23.76	8.51	0.0225

(b) MB Removal % and PTAC Yield

Figure 1 shows the three-dimensional (3D) response surfaces depicting how PTAC and PTAC fields remove MB to the power of the microwave radiation and the activation time. Based on Figure 1, the response of MB removal increased when both variables of radiation power and activation time increased. At a higher radiation power level, more volatile matter can be removed from the samples due to the volatilization process, thus, creating more pores. These pores create more sites for the adsorption process to occur, therefore, increasing the MB removal response. The volatilization process is prolonged at a high activation time, thus creating more pores and adsorption sites. Based on Figure 2, by increasing radiation power and radiation time, the response of PTAC yield decreased. At high radiation power and activation time, more volatile matter evaporated and left the sample, causing its weight to reduce [6,13].

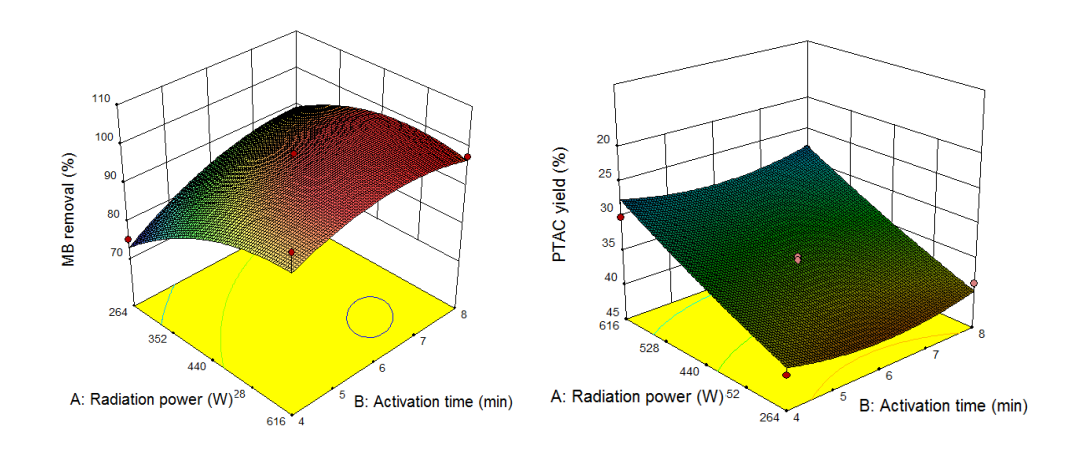


Figure 1: 3D surface plot of MB

Figure 2: 3D surface plot of PTAC

Characteristics of Samples

(a) Scanning Electron Microscopy (SEM) Analysis

PT and PTAC's respective surface morphologies are shown in Figure 3(a) and (b). In the imaging analysis, a similar activation process at a 1000x magnification scale has been used for comparison. According to Figure 3, the surface of the raw palm trunk is relatively flat and compact, and there are no noticeable cracks or crevices. In addition, pore blockage is caused by an agglomeration on its external surface, which can be caused by the presence of inorganic compounds in the carbon structure [14]. In contrast, the sponge-like structure of the SEM image of PTAC in Figure 3(b) is accompanied by cavities and cracks, comparable to the commercial activated carbon. The variation in shape and arrangement of pores in the SEM images of PT and PTAC demonstrates that the direct activation method is effective in producing porous carbon materials.

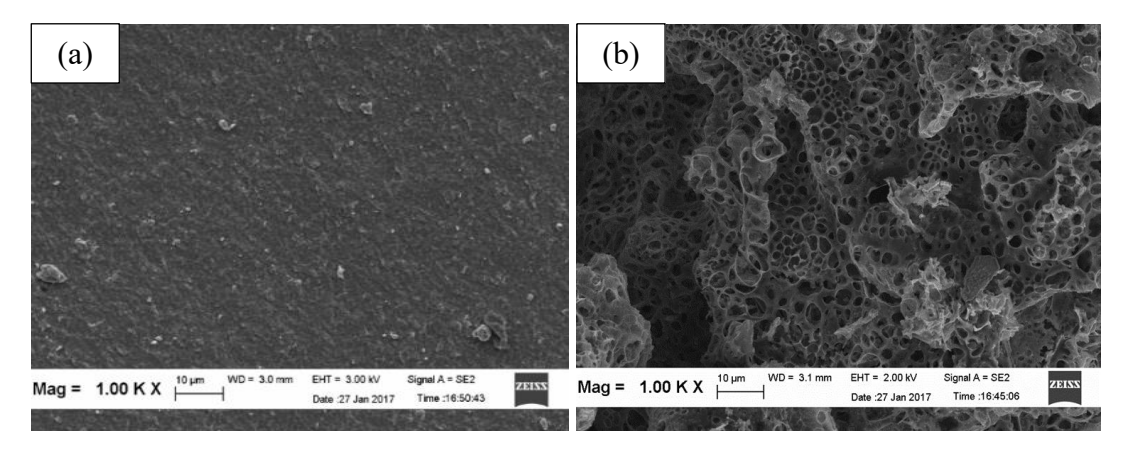


Figure 3: SEM images of (a) PT and (b) PTAC

(b) BET Surface Area and Pore Characterization

The samples were analyzed for their pore characteristics and surface area by activating the material in the microwave with CO₂ as the activating agent, which increases the PTAC's pore volume and surface area. The PTAC was found to have a high BET surface

area of 772.35 m²/g, total pore volume of 0.450 cm³/g, and average pore diameter of 3.88 nm (mesopores region). The PT has only a BET surface area of 2.12 m²/g, which is advantageous for dye adsorption. Additionally, by increasing the CO₂-carbon interaction, CO₂ gasification at high temperatures enhanced the carbon content and increased the number of pores in PTAC [15].

The SEM analysis, which revealed that PTAC has significantly superior textural properties to its parent material, is in line with the results obtained here. PTAC are categorized as mesoporous materials by the International Union of Pure and Applied Chemistry (IUPAC) because their average pore diameter is between 2 and 50 nm. During the activation process, non-carbon compositions like hydrogen and oxygen are released, causing the activated carbon to develop pores. After the Boudouard reaction Cs \rightarrow CO₂ + 2CO_g [13], the reaction between the carbon surface and CO₂ gas also accelerates the formation of the activated carbon's pore structure and texture

(c) Proximate and Elemental Analysis

The proximate analysis focused on the volatile matter, moisture content, fixed carbon, and ash value for both PT and PTAC. As a result, the fixed carbon increased while the ash, volatile matter, and moisture content decreased from PT to PTAC. The sample's total carbon content is reflected in the less volatile matter, which indicates that the carbonization process has been completed and left more fixed carbon in the sample [16]. The outcome from the primary examination displayed in Table 4 shows that the carbon component rate expanded from 30.84 % to 78.22 % while different components diminished. This is because a high carbon purity is produced when volatile compounds break down and organic substances break down by microwave irradiation.

Sample Proximate analysis (%) Elemental analysis (%) Volatile Moisture Fixed C Н $(N+O)^a$ Ash carbon PT 26.47 57.82 10.88 2.35 30.84 7.44 0.28 61.44 **PTAC** 14.19 5.74 74.30 1.91 78.22 1.82 0.15 19.81

Table 4: Proximate and Elemental Analysis

Batch Adsorption Studies

(a) Equilibrium Studies

i. Effect of Initial Dye Concentration and Contact time

Figure 4 illustrates the pattern of dye adsorption onto PTAC as a function of contact duration and starting dye concentration (25-300 mg/L) at 30 0 C. Initially, the adsorption uptake overgrew before decreasing gradually until equilibrium was attained. This event happens because the solute concentration gradient at the beginning of the reaction produces a significant driving force for dye molecules to connect to the PTAC active site. The gradual slowing of the adsorption rate on the PTAC towards the end of the experiment concludes that because there are no active sites on the adsorbent's surface, a monolayer of MB forms there once equilibrium has been established [17]. The absence of active sites created an

^a Estimated by difference

electrostatic barrier or repelling forces between the dye molecules and the adsorbent surface, making it difficult for the dye molecules to adhere to the adsorbent surface. We can conclude that adsorption equilibrium has been established when the rate at which molecules adsorb and desorb from a surface is equal [18,19]. Regarding contact time, it was observed that the greater initial concentration of dye required a longer contact time to reach equilibrium. In the last stages of the experiment, a balance was achieved. There was no change in the concentration of dye molecules on the solid surface or in the bulk solution. The dye molecules must first react with the boundary layer effect, diffuse from the film onto the adsorption sites, and diffuse into the adsorbent's porous structure [20]. Low-concentration dye molecules readily adhere to the adsorbent's external surface, speeding the adsorption process. During the process of adsorption, the exterior surface indirectly attains saturation. As there were just a few activity sites at this time, the molecules had to diffuse further into the interior pores of the PTAC. Due to this, a high initial concentration requires more time to attain equilibrium.

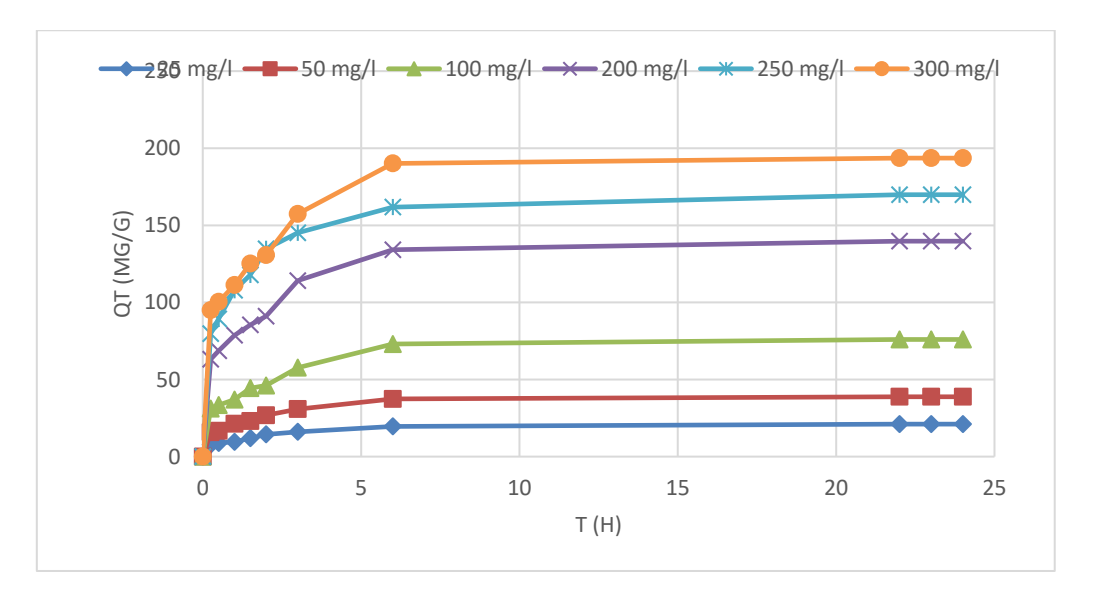


Figure 4: MB dye adsorption uptakes versus adsorption time at various initial dyes concentrations at 30 °C

ii. Effect of Solution Temperature

The temperature of the arrangement has a significant impact on adsorption efficiency. As a matter of fact, this meant that higher temperatures resulted in a greater capacity for adsorption. Initial MB concentration of 300 mg/L was used to study the effect of solution temperature. Adsorbed MB dye increased from 193.59 to 219.14 mg/g when solution temperature increased from 30 °C to 60 °C. The result provided evidence that the adsorption was an endothermic interaction. Figure 5 shows the starting dye concentrations for this study at various temperatures (30, 45, and 60 °C).

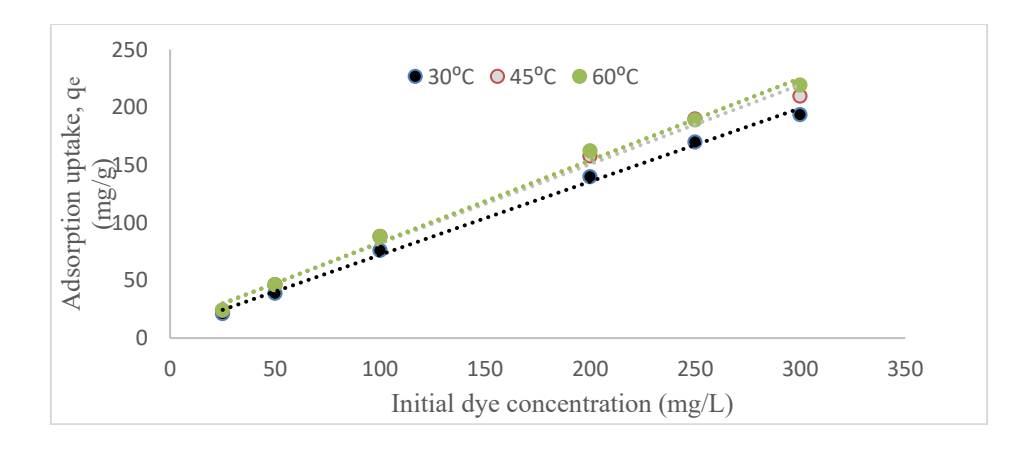


Figure 5: MB dye adsorption uptake versus initial dye concentration at different temperatures

(b) Adsorption Isotherms

Adsorption isotherms describe the adsorption condition when the process reaches equilibrium. This study employed the Temkin, Freundlich, and Langmuir adsorption isotherm models. Experimental data were used to select these models. The model's appropriateness was then determined by comparing each model's R^2 value to 1. As evidenced by the computed value R^2 in Table 5, the experimental data perfectly matched the following isotherm order. In this comparison, Freundlich outperformed Temkin ($R^2 = 0.985$) and Langmuir ($R^2 = 0.955$). These isotherms characterize the behavior of the MB dye multilayer adsorption process to illustrate the variability of the PTAC. PTAC successfully absorbs MB dye if and only if n is larger than or equal to 1 [19]. The non-ideal heterogeneous behavior of the adsorption process is further illustrated by the Freundlich isotherm.

Table 5: Isotherm parameters for MB removal at 30 °C

Langmuir	Freundlich	Temkin
$q_{\rm m} = 312.5$	$n_F = 1.44$	$B_T = 47.56$
$K_{L} = 0.014$	$K_F = 7.936$	$A_T = 1.152$
$R^2 = 0.955$	$R^2 = 0.996$	$R^2 = 0.985$

(c) Batch Kinetics Studies

The adsorption kinetics of MB dyes onto PTAC is the subject of batch kinetic studies, which make use of the pseudo-first-order and pseudo-second-order kinetic models. In this study, the adsorption kinetics were examined using the plots of pseudo-first-order and pseudo-second-order kinetic models.

$$ln(q_e - q_t) = lnq_e - k_1 t$$
(3)

By plotting a graph of $\ln (q_e-q_t)$ against t, the outcome is straight line with the slope of $-k_I$ and intercept of $\ln q_e$. to get the pseudo-first-order model (Equation 3) while for the pseudo-second-order model (Equation 4)

$$\frac{t}{q_{t}} = \frac{1}{k_{2}q_{e}^{2}} + \frac{1}{q_{e}}t\tag{4}$$

A graph of t/q_t against t gives a straight line with a slope of $1/q_e$ and an intercept of $1/k_2q_e^2$. Although the pseudo-first-order kinetic has an R^2 near 1, due to less error found in pseudo-second-order models. Details of the calculation are tabulated in Table 6.

C _o	Experimental Co data		Pseudo-first-order			Pseudo-second-order			
(mg/L)	q _e (mg/g)	k ₁ (hr ⁻¹)	q _e (mg/g)	R ²	k ₂ (g/mg.hr)	q _e (mg/g)	R ²		
25	21.08	0.3716	15.188	0.981	0.087	18.587	0.954		
50	38.81	0.3884	26.330	0.998	0.056	34.483	0.974		
100	75.97	0.3179	51.030	0.995	0.032	62.500	0.959		
200	139.73	0.3751	89.006	0.992	0.019	121.951	0.962		
250	169.86	0.4832	101.504	0.993	0.015	161.290	0.989		
300	193.59	0.3521	113.659	0.997	0.016	166.667	0.975		

Table 6: Kinetics parameters for MB removal at 30 °C

(d) Adsorption Thermodynamic Studies

Thermodynamics is studied to understand better how temperature affects the adsorption process. The slope created by this relationship provides the values of ΔH° and ΔS° . Equation 5 is also used to calculate the standard free energy change.

$$\Delta G^{\circ} = \Delta H^{\circ} - T \Delta S^{\circ} \tag{5}$$

Moreover, the Arrhenius activation energy, E_a obtained from Arrhenius equation (Equation 6) can make a graph of $\ln k_2$ versus $\ln T$.

$$\ln k_2 = \ln A - \frac{E_a}{RT} \tag{6}$$

where, k_2 = rate constant obtained from pseudo-second-order kinetic model (g/mg h); A= Arrhenius factor, E_a = Arrhenius activation energy of adsorption (kJ/mol), R = Universal gas constant (8.314 J/mol K) and T = Absolute temperature (K). The increased of ΔH° in MB adsorption were positive (34.48 kJ/mol) worth demonstrating that the process was endothermic. The fact that the adsorption capacity also increases as the solution's temperature rises is evidence of this endothermic process. During the adsorption process, a positive value for S° (0.13 kJ/mol.K) is obtained if there is an increase in random movement at the interface between the solid and the solution. This demonstrates the adsorbent's affinity for dye molecules. The adsorption process is spontaneous when ΔG° has a negative value (-5.22 at 303 K, -8.34 at 318 K, and -8.99 at 333 K). Additionally, the fact that the adsorption process was physisorption is evidenced by the fact that the obtained E_a value (7.33 kJ/mol) is lower than 42 kJ/mol [1].

Conclusions

In conclusion, the most important results are that the optimal microwave power and activation time for PTAC preparation were found to be 501 W and four minutes, respectively. Under these conditions, PTAC yielded 32.27 % and MB removal was 91.35 %. The BET surface area, total pore volume, and fixed carbon content of this sample are, respectively, 772.35 m²/g, 0.450 cm³/g, and 74.30 %. Based on SEM images, the surface morphology of precursor was found to be flat, compact and contain no pores. On contrary, the surface morphology of PTAC was seen to be filled with many pores. Compared to a low initial concentration, a high initial concentration of MB dye has a higher adsorption uptake. However, to reach equilibrium, it requires a longer contact time. The higher the solution temperature will further increase the adsorption equilibrium capacity. The Freundlich adsorption isotherm and pseudo-second-order kinetic models, respectively, were the most suitable adsorption isotherm and kinetic models for MB adsorption onto PTAC. MB dye adsorption onto PTAC was found to be an endothermic reaction in thermodynamic studies.

Acknowledgements

This research was funded by Ministry of Higher Education Malaysia through the Fundamental Research Grant Scheme (project code: FRGS/1/2021/TK0/USM/01/3).

Author Contributions

All authors contributed toward data analysis, drafting and critically revising the paper and agree to be accountable for all aspects of the work.

Disclosure of Conflict of Interest

The authors declare no potential conflict of interest in the publication of this work.

Compliance with Ethical Standards

The work is compliant with ethical standards.

References

- [1] Mohamad Yusop, M. F., Tamar Jaya, M. A., Idris, I., Abdullah, A. Z. & Ahmad, M. A. (2023). Optimization and Mass Transfer Simulation of Remazol Brilliant Blue R Dye Adsorption onto Meranti Wood Based Activated Carbon. *Arabian Journal of Chemistry*. 16(5), 104683.
- [2] Chan, L. S., Cheung, W. H., Allen, S. J. & McKay, G. (2012). Error Analysis of Adsorption Isotherm Models for Acid Dyes onto Bamboo Derived Activated Carbon. *Chinese Journal of Chemical Engineering*. 20(3), 535-542.

- [3] Dai, Y., Zhang, N., Xing, C., Cui, Q. & Sun, Q. (2019). The adsorption, regeneration and engineering applications of biochar for removal organic pollutants: A review. *Chemosphere*. 223, 12-27.
- [4] Yusop, M. F. M., Ahmad, M. A., Rosli, N. A., Gonawan, F. N. & Abdullah, S. J. (2021). Scavenging malachite green dye from aqueous solution using durian peel based activated carbon. *Malaysian Journal of Fundamental and Applied Sciences*. 17(1), 95-103.
- [5] Davarnejad, R., Afshar, S. & Etehadfar, P. (2020). Activated carbon blended with grape stalks powder: Properties modification and its application in a dye adsorption. *Arabian Journal of Chemistry*. 13(5), 5463-5473.
- [6] Firdaus Mohamad Yusop, M., Aziz, A. & Azmier Ahmad, M. (2022). Conversion of teak wood waste into microwave-irradiated activated carbon for cationic methylene blue dye removal: Optimization and batch studies. *Arabian Journal of Chemistry*. 15(9), 104081.
- [7] Ahmad, M. A., Eusoff, M. A., Oladoye, P. O., Adegoke, K. A. & Bello, O. S. (2021). Optimization and batch studies on adsorption of Methylene blue dye using pomegranate fruit peel based adsorbent. *Chemical Data Collections*. 32, 100676.
- [8] Ahmad, M. A., Ahmed, N. B., Adegoke, K. A. & Bello, O.S.(2021). Adsorptive potentials of lemongrass leaf for methylene blue dye removal. *Chemical Data Collections*. 31.
- [9] Li, S., Cho, M.-K., Lee, K., Deng, S., Zhao, L. & Yuan, X.(2022). Diamond in the rough: Polishing waste polyethylene terephthalate into activated carbon for CO2 capture. *Science of The Total Environment*. 834, 155262.
- [10] Yusop, M. F. M., Jaya, E. M. J. & Ahmad, M. A. (2022). Single-stage microwave assisted coconut shell based activated carbon for removal of Zn(II) ions from aqueous solution Optimization and batch studies. *Arabian Journal of Chemistry*. 15(8), 104011.
- [11] Yusop, M. F. M., Mohd Johan Jaya, E., Mohd Din, A. T., Bello, O. S. & Ahmad, M. A. (2022). Single-Stage Optimized Microwave-Induced Activated Carbon from Coconut Shell for Cadmium Adsorption. *Chemical Engineering & Technology*. 45(11), 1943-1951.
- [12] Jafri, N. H. S., Jimat, D. N., Azmin, N. F. M., Sulaiman, S. & Nor, Y. A. (2021). The potential of biomass waste in Malaysian palm oil industry: A case study of Boustead Plantation Berhad. *IOP Conference Series: Materials Science and Engineering*. 1192(1), 012028.
- [13] Elsayed, M. & Abuzalat, O. (2015). Factor Affecting Microwave Assisted Preparation of Activated Carbon from Local Raw Materials. *International Letters of Chemistry, Physics and Astronomy*. 47, 15-23.
- [14] Khasri, A. & Ahmad, M. A.(2018). Adsorption of basic and reactive dyes from aqueous solution onto Intsia bijuga sawdust-based activated carbon: batch and column study. *Environmental Science and Pollution Research*. 25(31), 31508-31519.

- [15] Ahmad, A. A., Ahmad, M. A., Yahaya, N. K. E. M. & Karim, J. (2021). Adsorption of malachite green by activated carbon derived from gasified Hevea brasiliensis root. *Arabian Journal of Chemistry*. 14(4).
- [16] Malik, R., Mukherjee, M., Swami, A., Ramteke, D. S. & Sarin, R. (2004). Validation of Adsorption Efficiency of Activated Carbons through Surface Morphological Characterization Using Scanning Electron Microscopy Technique. *Carbon letters*. 5, 75-80.
- [17] Pathania, D., Sharma, S. & Singh, P. (2017). Removal of methylene blue by adsorption onto activated carbon developed from Ficus carica bast. *Arabian Journal of Chemistry*. 10, S1445-S1451.
- [18] Almeida, C. A. P., Debacher, N. A., Downs, A. J., Cottet, L. & Mello, C. A. D. (2009). Removal of methylene blue from colored effluents by adsorption on montmorillonite clay. *Journal of Colloid and Interface Science*. 332(1), 46-53.
- [19] Mohamad Yusop, M. F., Nasehir Khan, M. N., Zakaria, R., Abdullah, A. Z. & Ahmad, M.A. (2023). Mass transfer simulation on remazol brilliant blue R dye adsorption by optimized teak wood Based activated carbon. *Arabian Journal of Chemistry*. 16(6), 104780.
- [20] Hameed, B. H. (2009). Grass waste: A novel sorbent for the removal of basic dye from aqueous solution. *Journal of Hazardous Materials*. 166(1), 233-238.